Mineralogical Magazine (2021), **85**, 132–141
doi:10.1180/mgm.2020.105

CAMBRIDGE UNIVERSITY PRESS

Article

Novograblenovite from Radlin, Upper Silesia, Poland and its relation to 'redikortsevite'

Jan Parafiniuk[1], Marcin Stachowicz[1]* and Krzysztof Woźniak[2]

[1]Institute of Geochemistry, Mineralogy and Petrology, Faculty of Geology, University of Warsaw, Żwirki i Wigury 93, 02-089 Warsaw, Poland; and [2]Department of Chemistry, University of Warsaw, Pasteura 1, 02-093 Warszawa, Poland

Abstract

The paper presents detailed mineralogical and structural characteristics of novograblenovite that occurs abundantly on a burning coal dump at Radlin, Upper Silesia, Poland. Our results indicate that $NH_4MgCl_3{\cdot}6H_2O$ is the proper formula of this mineral. The thermal behaviour of novograblenovite shows a two-step dehydration at 155 and 193°C and sublimation of NH_4Cl at 341°C. A Raman spectrum, obtained for the first time, reveals the normal modes of H_2O and NH_4^+ vibrations. The crystal structure of novograblenovite was refined on the basis of high quality X-ray diffraction data. The final discrepancy factor wR_2 was 0.0567 for 94 parameters and 1464 independent reflections. The structure has a monoclinic *C*2/*c* space group symmetry with the following unit cell parameters: $a = 9.2709(3)$ Å, $b = 9.5361(2)$ Å, $c = 13.2741(4)$ Å and $\beta = 90.054(3)°$. We were able to specify the architecture of the disordered NH_4^+ cation located at the symmetry centre. This led to reasonable parameters for the H-bonding formed by this cation. In carnallite the K^+ cations occupy an identical space to the ammonium ion in novograblenovite, but when embedded into the latter crystal structure it is bound less tightly. Voids occupy 14% of the space in the novograblenovite crystal structure. Novograblenovite is exactly the same phase as the 'redikortsevite' described previously from Chelabinsk coal dumps and this informally introduced name should be abandoned.

Keywords: burning coal dumps, ammonium mineral, crystal structure, differential thermal analysis, Raman spectroscopy, novograblenovite

(Received 15 July 2020; accepted 23 December 2020; Accepted Manuscript published online: 5 January 2021; Associate Editor: Mihoko Hoshino)

Introduction

A recent description of a new mineral, novograblenovite, with the formula $(NH_4,K)MgCl_3{\cdot}6H_2O$ was published by Okrugin *et al.* (2019). The mineral name was approved by the Commission on New Minerals, Nomenclature and Classification (CNMNC) of the International Mineralogical Association (IMA) as IMA2017-060 (Okrugin *et al.*, 2017). The mineral was named after P. I. Novograblenov (1892–1934), a naturalist and researcher of the Kamchatka Peninsula, Russia. Novograblenovite was found on a basaltic lava of the Tolbachik fissure eruption as a product of volcanic exhalation. In their paper Okrugin *et al.* noted that they were informed by an anonymous member of the CNMNC that novograblenovite is "likely to be very close to redikortsevite", found among exhalative products on the burning coal dump near Chelabinsk, Southern Ural, Russia. The name 'redikortsevite' was introduced by Chesnokov *et al.* (1988) after I. I. Redikortsev, the discoverer of the Chelabinsk coal basin. However, their proposal has never been submitted to the Commission for approval (Jambor and Puziewicz, 1993) and 'redikortsevite', although informal, still exists in the mineralogical literature.

'Redikortsevite' is another example following 'lesukite', steklite and other cases, where the phase found on the burning coal dumps was accepted as a valid mineral only after finding it in a similar environment due to volcanic exhalation. In all these cases the minerals formed on the coal heaps are better developed and occur in bigger amounts than in the volcanic exhalations.

A significant amount of the phase under discussion was found among exhalation products of an underground fire on a dump at Radlin near Rybnik, Upper Silesian coal basin, Poland. In 2015 we submitted this case to the CNMNC for acceptance as a new mineral under the already existing name 'redikortsevite'. In doing so we opened a debate on changing the commission policy for combustion products forming on burning coal-dumps. Consequently, mineral products of spontaneously induced fires, without human ignition, when they form non-anthropogenic material, meet the general criteria for minerals and should be regarded as such (Parafiniuk and Hatert, 2020).

In this work, we present the results of investigations of 'redikortsevite' from Poland and aim to show that our material is essentially the same mineral as 'redikortsevite' of Chesnokov *et al.* (1988) from the Chelabinsk Coal Basin and the novograblenovite of Okrugin *et al.* (2019) from Kamchatka Peninsula and so should be described as novograblenovite. Therefore, the name 'redikortsevite' should be abandoned. The same opinion was recently expressed by Zolotarev *et al.* (2019) who re-examined materials from the Chesnokov study deposited in the Natural Science Museum in Miass, Russia. These authors referred to it as 'redikortsevite' to express the technogenic origin with respect to novograblenovite, a distinction that is no longer needed. Here, we complement the information on the crystal structure

*Author for correspondence: Marcin Stachowicz, Email: marcin.stachowicz@uw.edu.pl
Cite this article: Parafiniuk J., Stachowicz M. and Woźniak K. (2021) Novograblenovite from Radlin, Upper Silesia, Poland and its relation to 'redikortsevite'. *Mineralogical Magazine* **85**, 132–141. https://doi.org/10.1180/mgm.2020.105

from high quality single-crystal X-ray diffraction (XRD) data. In order to better understand the bonding interactions of mutually substituting NH_4^+/K^+ ions with the host lattice, an ionic Hirshfeld surface analysis has been undertaken using the program *CrystalExplorer* (Turner *et al.*, 2017).

In the Hirshfeld surface approach, electron density is divided into atomic fragments using the Stockholder partitioning concept, where weight function is defined as $w(\mathbf{r}) = \rho_{promolecule}/\rho_{procrystal}$. The $\rho_{promolecule}$ electron density is a sum of spherically averaged atomic electron densities of a given fragment, i.e. NH_4^+ or K^+. The $\rho_{procrystal}$ is the sum of spherical atomic densities of the surrounding crystal (Clementi and Roetti, 1974). This simple scalar function is highly localised to the molecule of interest, flat across the molecule itself with $w(\mathbf{r}) > 0.9$, and decaying rapidly to values < 0.1, with contours closely spaced around the molecule in the vicinity of the van der Waals surface. An isosurface of $w(\mathbf{r}) = 0.5$ is defined as the Hirshfeld surface. This special value defines the volume of space where the promolecule electron density exceeds that from all remaining atoms in the crystal structure. (Spackman and Jayatilaka, 2009; Spackman, 2013).

This is a much less time-consuming alternative to Bader's quantum theory of atoms in molecules space partitioning method (Bader, 1994) that we utilised for fluorite (Stachowicz *et al.*, 2017) with an extension of the procrystal electron density for aspherical atomic contributions (Coppens, 1997). The latter approach, although computationally demanding, allows for a more detailed analysis of electron density distribution and corresponding physico-chemical properties.

The procrystal electron density can also be utilised to visualise voids by identification of those parts of minerals or crystalline materials in general where the electron density is the smallest. Computation of this electron density is undertaken using *CrystalExplorer* software, by applying a 0.002 au cut-off (0.013 $e^-\cdot Å^{-3}$). The choice of 0.002 au results from early work by Bader *et al.* (1967) who verified that the 0.002 au contour is a physically reasonable measure of the molecular electron density, utilising over 95% of total electron density. This void representation was proposed by Turner *et al.* (2011). The authors compared it to the earlier outcomes by using a probe sphere of a given radius (commonly 1.2 Å), rolling over van der Waals surfaces of atoms in the crystal lattice, giving solvent accessible or solvent excluded regions (Spek, 2003). A big advantage of the proposed idea is the rapid calculation and visualisation of smooth void surfaces, their area and volume providing insight into their location and magnitude.

We also present chemical, thermal and Raman spectroscopy studies on novograblenovite from burning coal dumps, with the conditions of formation resulting in the finest novograblenovite crystal aggregates known so far (Fig. 1 and 2).

Mode of occurrence

A significant locality for novograblenovite is a burning coal-dump at Radlin, Rybnik area, Upper Silesian Coal Basin, Southern Poland, with the coordinates: 50°02'28.0"N and 18°28'36.6"E. This mineral forms as a sublimate around vents of hot gases escaping from the underground fire at the dump's surface. The temperature of the fire vapours containing an abundance of chlorides near the dump surface is estimated as *ca.* 250–300°C. Fire gases carry many mineral compounds (Kruszewski *et al.*, 2018) and after cooling on the dump surface produce a rich assemblage of exhalative minerals. Novograblenovite is one of the last

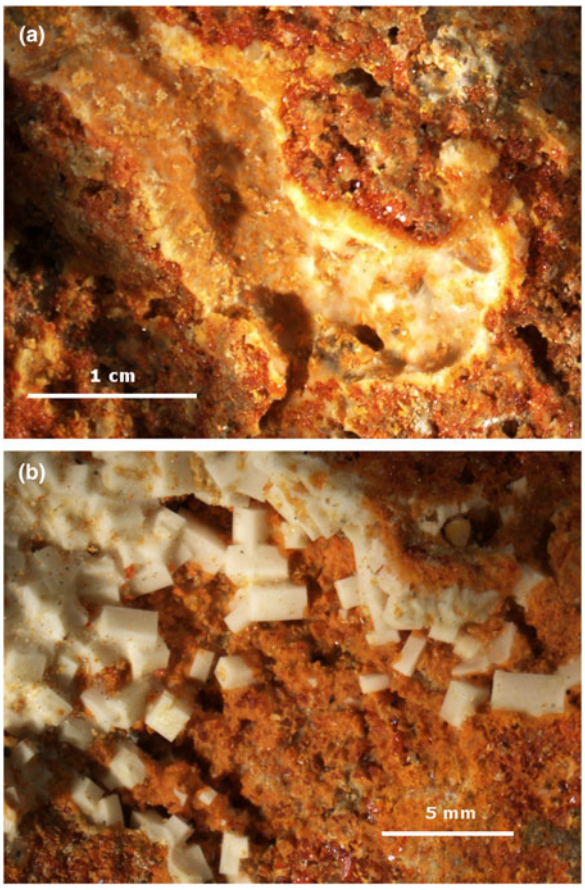

Fig. 1. White accumulation of novograblenovite surrounding inner surfaces of gas vents. (a) The outer orange parts of the accumulation are formed by kremersite; and (b) white, stubby crystals of novograblenovite, the largest known for this mineral.

minerals crystallising from vapours after the accumulation of more abundant kremersite $(NH_4)_2FeCl_5\cdot H_2O$. Associate chloride or sulfate minerals tend not to be in a direct paragenetic connection with novograblenovite and occur in different parts of sublimate accumulations. They comprise, besides kremersite, salammoniac NH_4Cl, cadwaladerite $Al_2Cl(OH)_5\cdot 2H_2O$, halite NaCl and possibly other, not yet specified, chlorides of Al and Fe. Granular or fibrous masses of novograblenovite build the inner parts of sublimates formed around the vents and their crystallisation temperature was slightly above 100°C. The sublimates may form porous crust accumulations up to a few cm thick and a few dozen cm wide, sometimes cementing fragments of rocks on or near the dump surface. The crust accumulations are irregularly pierced by channels or holes, oval in section, of a millimetre to 1–2 cm in diameter, which mark the traces of escaping gases. The walls of these channels are usually smooth with crystal individuals developing outwards from them (Fig. 1a).

The chloride sublimates are very similar to the so-called sulfate crusts composed of godovikovite, millosevichite, tschermigite and other sulfates, described from many underground coal fire and burning coal dumps (Žáček and Ondruš, 1997; Sindern *et al.*, 2005; Stracher *et al.*, 2005). However, besides the common presence of salammoniac efflorescences elsewhere, the formation of chloride crusts is much rarer than sulfate crusts. Rich, well developed chloride crusts have so far been found only in Chelabinsk Coal Basin, Southern Urals, Russia and Rybnik area, Upper Silesia Coal Basin, Poland. Their origin could probably be

https://doi.org/10.1180/mgm.2020.105 Published online by Cambridge University Press

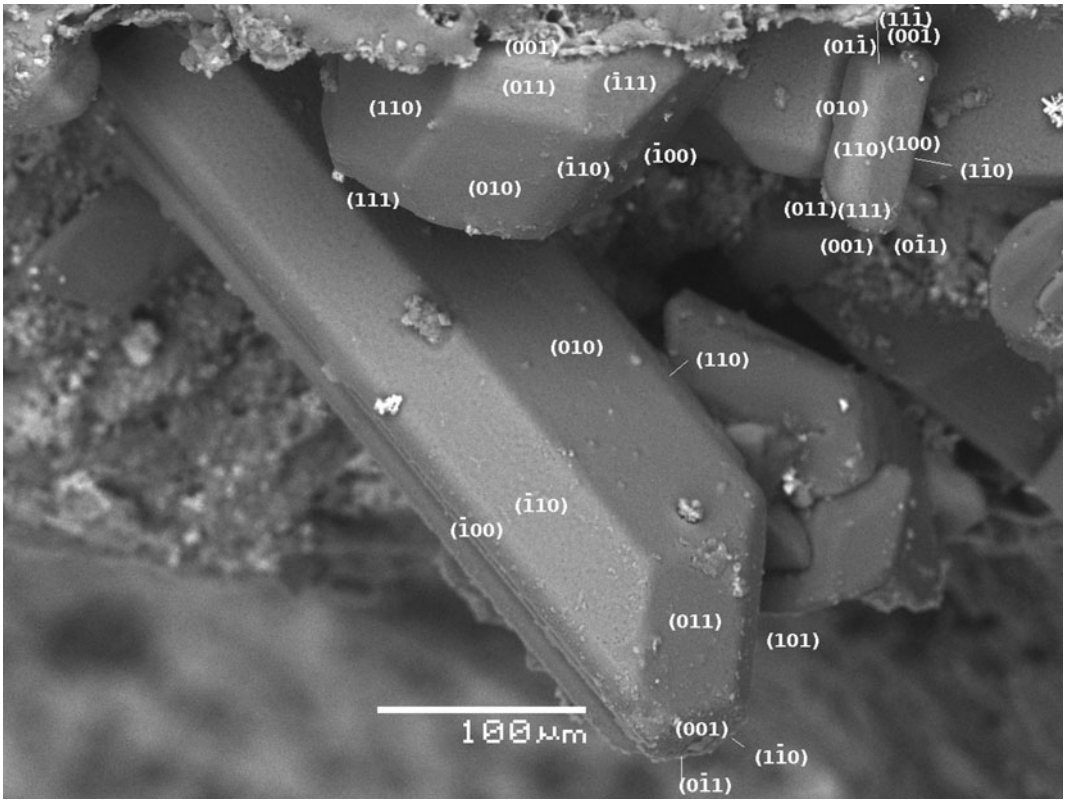

Fig. 2. SEM image of prismatic well developed crystals of novograblenovite.

explained by the elevated salinity of the Carboniferous strata and underground waters influenced by younger, close lying, evaporates. In the Upper Silesian Coal Basin, these chloride sublimates were found in its southern part which is close to the area where Miocene evaporates were deposited. Similarly the Chelabinsk area is close to the occurrence of Permian evaporates of Southern Urals.

Novograblenovite at Radlin occurs as white, or yellowish to orange crystal masses up to a few cm in diameter, stained by kremersite inclusions. The surface of novograblenovite has accumulations of well developed, white stubby or transparent, prismatic, fine crystals (Figs 1b, 2). The size of the biggest, cuboid, crystals is up to 1 mm. Perfectly developed colourless and transparent monocrystals are a tenth of a millimetre in size. The mineral is brittle, soft (hardness ≈ 2 on the Mohs scale). Crystals have a vitreous lustre, white streak and are non-fluorescent. Cleavage or parting was not observed. Novograblenovite is very soluble in water but less deliquescent than its potassium analogue – carnallite; thus it may be preserved for years in dry ambient conditions.

The appearance, physical properties and occurrence of novograblenovite from Radlin are analogous to the 'redikortsevite' of Chesnokov *et al.* (1988). In both localities minerals form similar exhalative accumulations with kremersite ('kopeiskite' in the Chesnokov *et al.*, 1988 nomenclature). The appearance of novograblenovite from burning coal dumps is rather different from its occurrence in volcanic exhalations in Kamchatka where it forms tiny needle-like crystals or fibrous aggregates together with gypsum and halite in basalt cavities (Okrugin *et al.*, 2019). The physical properties of the mineral from all these localities are completely compatible. The only small difference is in the density. Chesnokov *et al.*'s (1988) measurement gave 1.43(1) g·cm^{-3}. The densities calculated from single-crystal X-ray diffraction experiments are 1.453 g·cm^{-3} (this study) and 1.504 g·cm^{-3} (Okrugin *et al.*, 2019). This difference may be explained by slightly different compositions of the material under study.

Experimental methods

Observations of the crystal morphology of novograblenovite and a preliminary determination of its composition were carried out by scanning electron microscopy (SEM) using a JEOL JSM-680LA microscope equipped with a Bruker XFlash 6/10 EDS attachment. Because the mineral is very unstable under the electron beam, our chemical analyses were performed using wet chemical methods. Concentrations of K^+, Na^+, Mg^{2+}, Ca^{2+}, Al^{3+}, total Fe, Mn^{2+} were determined by inductively coupled plasma optical emission spectrometry (ICP–OES) with the Optima 5300 DV Perkin Elmer apparatus. For analysis of NH_4^+, Cl^-, SO_4^{2-} we used ICP–OES and water contents were determined from TG curves obtained by thermogravimetric analysis.

A 25 mg sample of novograblenovite was prepared for thermogravimetric analysis. The analysis was carried out on a SDT Q600 V20.5 Build 20 apparatus of V4 5A TA Instruments. The ramping temperature was set to 10°C per minute and heating was performed in the range 25 to 1000°C. Nitrogen flow was set to 30 mL/min.

Raman spectra were recorded using a Labram HR800 (Horiba Jobin Yvon) spectrometer, coupled with a confocal microscope, working in a back-scattering configuration. Spectra were obtained using 100× magnification Olympus objectives. The instrument was equipped with a Peltier-cooled CCD detector (1024 × 256 pixels).

https://doi.org/10.1180/mgm.2020.105 Published online by Cambridge University Press

The frequency doubled Nd:YAG laser (532 nm) with a power at a sample from 0.2 to 2 mW was used as the excitation source. Raman data was acquired with the 1800 grooves/mm holographic grating. The confocal pinhole size was set to 200 μm. The spectra were accumulated within from 10 to 15 scans, the integration time ranged from 150 to 300 s. A calibration of the instrument was performed before each batch experiment with the 520 cm^{-1} band of the polished Si wafer.

For the structural study, a suitable crystal 0.24 mm × 0.24 mm × 0.20 mm was mounted on a Mitegen loop support on a KUMA KM4CCD κ-axis diffractometer equipped with Opal CCD detector and graphite-monochromated Mo*Kα* radiation. The crystal was kept at a steady 100(2) K temperature during data collection. Data were measured using *ω* scans. The total number of runs and images was based on the strategy calculation from the program *CrysAlisPro* (Agilent, V1.171.35.7, 2011). The full Ewald sphere data were collected to θ = 26.32° resolution. Data reduction, scaling and multi-scan absorption corrections using spherical harmonics as implemented in *SCALE3 ABSPACK* were performed using *CrysAlisPro* (Agilent, V1.171.35.7, 2011). The structure was solved with the *ShelXS* (Sheldrick, 2008) using the Direct Methods with *Olex2* (Dolomanov *et al.*, 2009) as the graphical interface. The model was refined with version 2014/7 of *ShelXL* (Sheldrick, 2015) using least squares minimisation. The crystallographic data and refinement details of the final model of the crystal structure are presented in Table 1. The crystallographic information file has been deposited with the Principal Editor of *Mineralogical Magazine* and is available as Supplementary material (see below).

Table 1. The crystal information and details of X-ray diffraction data collection and refinement for novograblenovite from Radlin.

Crystal data	
Ideal formula	$NH_4MgCl_3·6H_2O$
Crystal dimensions (mm)	0.24 × 0.24 × 0.2
Crystal system, space group	Monoclinic, *C*2/*c*
Temperature (K)	100(2)
a, *b*, *c* (Å)	9.2709(3), 9.5361(2), 13.2741(4)
β (°)	90.054(3)
V (Å^3)	1173.53(7)
Z	4
Calculated density (g cm^{-3})	1.453
μ (mm^{-1})	0.826
Data collection	
Crystal description	Colourless block
Instrument	KUMA KM4 CCD Opal
Radiation type, wavelength (Å)	Mo*Kα*, 0.71073
Number of frames	646
θ range (°)	3.0583, 28.6976
Absorption correction	Multi-scan (*ABSPACK*; *CrysAlis PRO*, Agilent Technologies, Version 1.171.35.7)
T_{min}, T_{max}	0.991, 1.000
No. of measured, independent and observed [I >2σ(I)] reflections	25255, 1464, 1290
Data completeness to 26.32° θ (%)	99.77
Graphite monochromator	R_{int} = 0.0259
Indices range of *h*, *k*, *l*	$-12 \le h \le 12$, $-12 \le k \le 12$, $-17 \le l \le 17$
Refinement details	
Refinement	Full-matrix least squares on F^2
Number of reflections, parameters, restraints	1464/94/21
R_1 [$I > 2\sigma(I)$], R_1(all)	0.0216, 0.0271
wR_2 [$I > 2\sigma(I)$], wR_2(all)	0.0534, 0.0568
GoF	1.128
$\Delta\rho_{max}$, $\Delta\rho_{min}$ (e$^-$ Å^{-3})	0.19, −0.34

Results and discussion

Composition of novograblenovite

Results of all available chemical analyses of novograblenovite are collected in Table 2. The composition of 'redikortsevite' from Chelabinsk analysed by Chesnokov *et al.* (1988) was obtained by unspecific, presumably wet chemical, methods. Novograblenovite from Kamchatka was analysed on unpolished surfaces using SEM energy dispersive spectroscopy (EDS). This method was also applied by Zolotarev *et al.* (2019) for re-examination of Chesnokov's material. As discussed by these authors EDS analysis in this case, performed both on unpolished and polished surfaces, carries some uncertainty. Mineral samples cannot be analysed by the wavelength dispersive spectroscopy method because they evaporate quickly even under low voltage and with a wide electron beam. The mineral is also destroyed during polishing – required for the microprobe technique. Our wet chemical methods are more precise but require pure mineral samples, almost impossible to prepare in the case of novograblenovite. Even carefully selected samples contain a small admixture of kremersite and gypsum. Thus, at the very least iron, calcium and sulfate contents should not be included in the chemical formula of novograblenovite.

The results of three analyses from this study and the very similar data of Chesnokov *et al.* (1988) and Zolotarev *et al.* (2019)

Table 2. Chemical analyses of novograblenovite (in wt.%).

		Radlin			Chelyabinsk		
Constituent	$NH_4MgCl_3·6H_2O$	1	2	3	A	B	Kamchatka
NH_4^+	7.01	8.03	6.83	6.84	5.84		
K^+			0.47	0.48	<0.10		6.7
Na^+		0.53	0.30	0.55	<0.10		
Mg^+	9.47	6.75	8.25	7.62	7.72	9.41	9.3
Ca^{2+}		1.50	0.03	0.05	0.43		
Fe (total)		1.82	0.15	0.93	1.78		
Mn^{2+}		0.18	0.04	0.05	0.09		
Al^{3+}		0.36	0.01	0.01	0.80		
Cl^-	41.44	43.04	45.27	47.16	39.21	42.34	34.5
SO_4^{2-}		4.50	0.15	0.83			
H_2O	42.08	32.53[1]	39.38	37.59	42.15	41.93	
Total	100.00	100.00	100.88	102.11	98.02	100.00	89.5

[1]by difference; A – from Chesnokov *et al.* (1988); B – from Zolotarev *et al.* (2019)

https://doi.org/10.1180/mgm.2020.105 Published online by Cambridge University Press

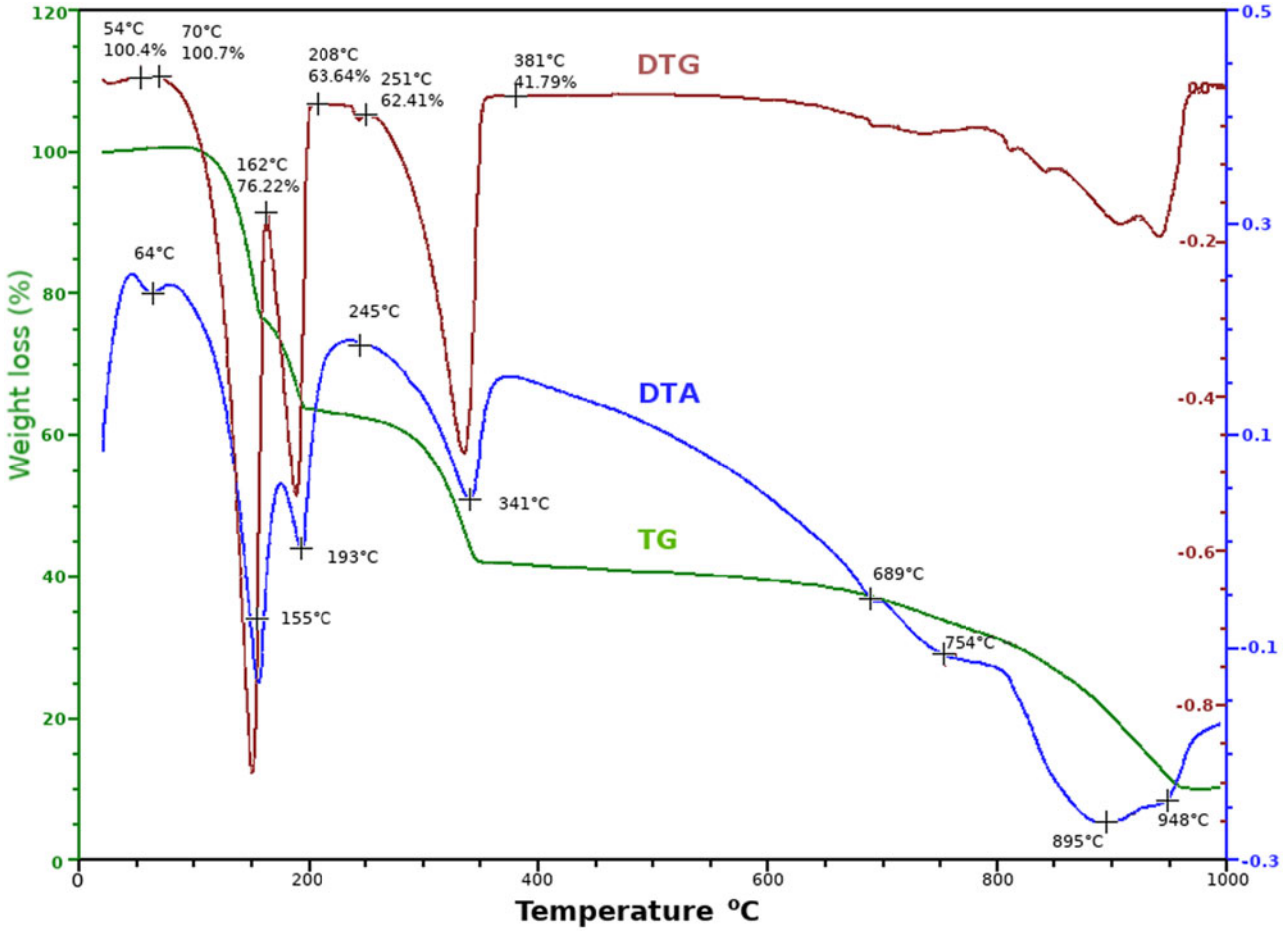

Fig. 3. Comparison between the TG, the TG first derivative (DTG) and DTA curves of novograblenovite from Radlin.

clearly indicate that the ideal formula of novograblenovite is $NH_4MgCl_3{\cdot}6H_2O$. Materials from burning coal-dumps do not contain the potassium detected in the mineral from Kamchatka. The relationship between the structure topology and the ionic radii of X^+ in the compounds of $XMgCl_3{\cdot}6H_2O$ type are discussed by Zolotarev *et al.* (2019).

The compositions of available novograblenovite samples shed light on the problem of the mineral's origin. Okrugin *et al.* (2019) stated that it was formed from volcanic gases enriched in NH_3 and HCl, whereas K and Mg are leached from basalt treated by volcanic exhalation. Novograblenovite from the burning coal dumps is of fully exhalative origin. In the chloride crusts magnesium, iron and aluminium come from volatile compounds, probably as metal chlorides from the fire centre. Gaseous products condensing on or near the dump surface were not affected by rock material on the visible scale.

Thermal data

The thermal decomposition of novograblenovite registered by the derivatographic method using thermogravimetric (TG) and differential thermal analysis (DTA) is shown in Fig. 3. DTA reveals two steps of dehydration with peaks at 155 and 193°C, respectively. The first peak, reflecting a drop of 23.8 wt.% on TG, corresponds to a loss of four water molecules from the formula unit. The second dehydration results in a loss of 12.7 wt.% which corresponds to an escape of the remaining two water molecules. The third peak on DTA curve at temperature of 341°C corresponds to sublimation of ammonium chloride with mass loss of 21.7 wt.%. The remaining magnesium chloride starts to decompose or/and escape above 700°C. Our results on the thermal decomposition of novograblenovite are significantly lower than those reported by Chesnokov *et al.* (1988) for 'redikortsevite'. The temperatures of dehydration of Chesnokov *et al.*, estimated at 315 and 395°C, are certainly too high for this easily dehydrated phase. Lower temperatures of dehydration for novograblenovite were reported recently by Zolotarev *et al.* (2019). Their high-temperature XRD experiments indicate that novograblenovite is stable to *ca.* 90°C, above which it transforms to another phase $NH_4MgCl_3{\cdot}2H_2O$, which is in agreement with our first step of dehydration. This phase is stable up to 140°C where the second step of dehydration begins. In the temperature range 160–370°C Zolotarev *et al.* (2019) observed no further diffraction from the sample on the high-temperature XRD patterns. Above 370°C they noticed the appearance of broad reflections of periclase, MgO.

Raman spectroscopy

The Raman spectrum of novograblenovite is shown in Fig. 4. The normal vibrational modes of H_2O molecules are at 3430 cm^{-1} (symmetric stretching ν_1) and at 1645 cm^{-1} (bending O–H deformations ν_2) (Hornig *et al.*, 1958; Haas and Hornig, 1960). The water

https://doi.org/10.1180/mgm.2020.105 Published online by Cambridge University Press

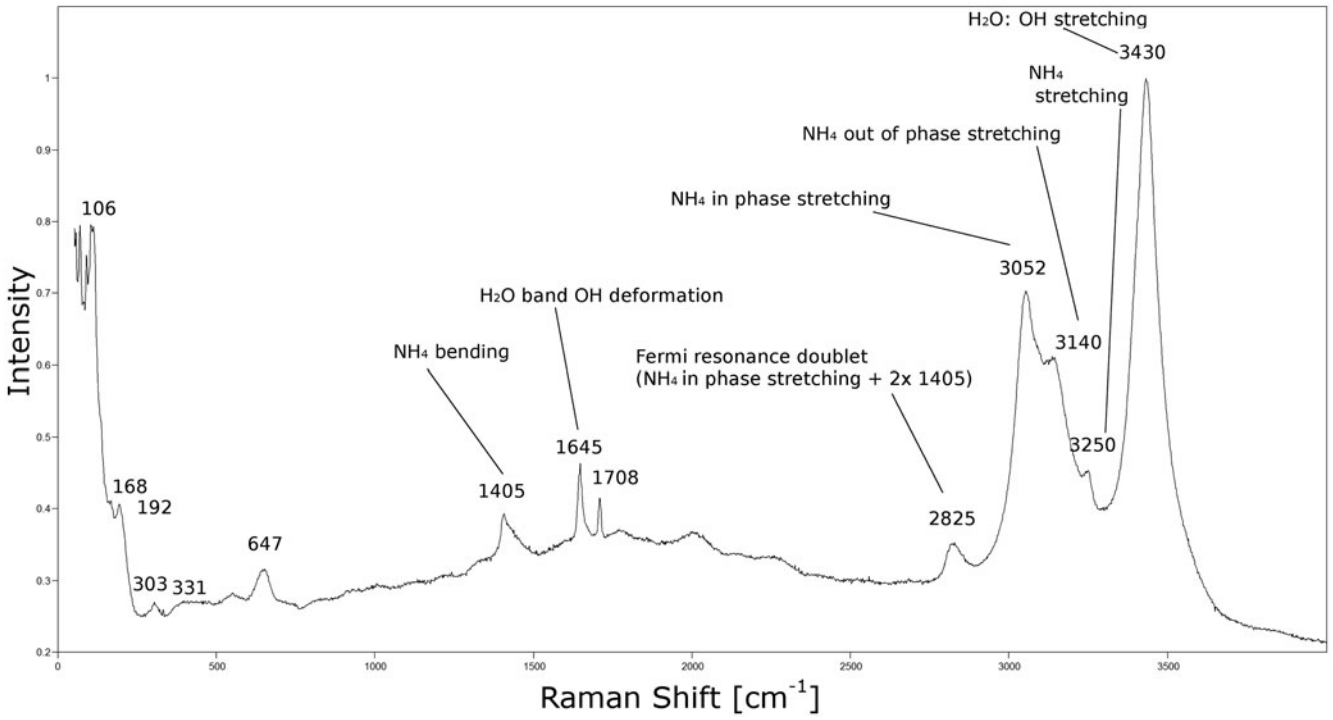

Fig. 4. Raman spectrum of novograblenovite from Radlin.

bending modes shift to higher frequencies by 50 cm^{-1} compared to the gas phase, from 1595 cm^{-1} in a magnesium hexaaquo complex (Chang and Irish, 1973) of novograblenovite. Furthermore, peaks at 647 cm^{-1} and 303 cm^{-1} are weak libration frequencies of water molecules in a $[Mg(H_2O)_6]^{2+}$ complex, H-bonded with Cl^- (Falk and Knop, 1973; Pye and Rudolph, 1998). Normal modes of the NH_4^+ ion are found at 3050 cm^{-1} for ν_1 in phase stretching, 1708 cm^{-1} for ν_2 doubly degenerate bending, 3140 cm^{-1} for ν_3 out of phase stretching and 1405 cm^{-1} for ν_4 triply degenerate bending (Nakamoto, 2008). The peak at 2825 cm^{-1} is a Fermi resonance doublet of overtone $2\nu_4$ with ν_1 normal mode (Larkin, 2011). The band at 3250 cm^{-1} (Majzlan *et al.*, 2013; Pekov *et al.*, 2014) corresponds to NH_4^+ stretching vibrations. Frequencies below 303 cm^{-1} denote crystal lattice vibrations.

Crystal structure

Novograblenovite from Radlin like the holotype (Okrugin *et al.*, 2019) crystallises in the monoclinic system, space group *C*2/*c* with $\beta = 90.054(3)°$ and 90.187(2)°, respectively. According to our data and those of Zolotarev *et al.* (2019), 'redikortsevite' was erroneously assigned to the orthorhombic system by Chesnokov *et al.* (1988). The crystal structure of the synthetic analogue (Solans *et al.*, 1983; Marsh, 1992) also indicates the monoclinic system to be correct for this mineral.

The list of atomic coordinates together with atomic, equivalent isotropic displacement parameters and anisotropic displacement parameters is given in Table 3. The contents of the independent part of the unit cell are shown in Supplementary Fig. 1.

The crystal structure can be divided into two subunits organised in a $CaTiO_3$ perovskite-type arrangement. The framework consists of corner sharing Cl^- octahedra with an NH_4^+ central ion, while the $[Mg(H_2O)_6]^{2+}$ coordination octahedra located in the structural cavities are essentially regular and stabilised by the O–H···Cl hydrogen bonds (Fig. 5). Carnallite, the potassium analogue to novograblenovite, despite having a similar chemical formula, $KMgCl_3{\cdot}6(H_2O)$, has a significantly different structure topology. It crystallises in the higher symmetry orthorhombic *Pnna* space group (Schlemper *et al.*, 1985). The three dimensional framework consists of two types of KCl_6 octahedra, of which ⅓, namely $K1Cl_6$ share corners with adjacent, more distorted $K2Cl_6$ octahedra, that share one face with another K2 octahedron. Openings around face-sharing octahedra are filled with $Mg(H_2O)_6$ and stabilised by a network of hydrogen bonds formed with chloride anions (Schlemper *et al.*, 1985; Okrugin *et al.*, 2019).

The crystal structures of synthetic samples of $(NH_4,K)MgCl_3{\cdot}6H_2O$ have missed the hydrogen atoms in their models (Solans *et al.*, 1983; Marsh, 1992). The N position in the novograblenovite of Okrugin *et al.* (2019) is occupationally disordered with K in a ratio of 2:1. The crystal analysed by Zolotarev *et al.* (2019) was non-merohedrally twinned. Both groups positioned the N atom on a two-fold symmetry axis which also constrained the positions of bonded H atoms. Crystals from Radlin analysed in this work are of exceptional quality compared to all studied previously. They are not affected by twinning or occupational disorder that deteriorate the accuracy of the final crystal structure model. Releasing the N atom from a symmetry element allowed a flexible reorientation of NH_4^+ inside a cage of 6 Cl^- vertices (Fig. 6) and decreased the anisotropic displacement parameters giving a better fit to the collected X-ray intensities.

We recognised that the N–H···Cl1 hydrogen bond, measured as a *D*···*A* distance is actually the shortest of all of these kinds of interactions in the crystal structure of novograblenovite (Table 4). The weighted residual factor wR_2 presents a divergence of the refined crystal structure model from all recorded X-ray scattering intensities. In this study the discrepancy factor wR_2= 5.7% is improved over twice with respect to Okrugin *et al.* (2019), wR_2=12.3% and 3 times compared to Zolotarev *et al.* (2019), wR_2=19.1%.

https://doi.org/10.1180/mgm.2020.105 Published online by Cambridge University Press

Table 3. Fractional atomic coordinates and displacement parameters (Å^2) for novograblenovite.

	x/a	*y/b*	*z/c*	U_{iso}*/U_{eq}	U^{11}	U^{22}	U^{33}	U^{12}	U^{13}	U^{23}
Cl1	½	½	½	0.02216(11)	0.01354(18)	0.01362(19)	0.0393(2)	−0.00001(11)	0.00052(16)	0.00845(13)
Cl2	0.74000(3)	0.75707(2)	0.25423(2)	0.01566(9)	0.02003(15)	0.01459(15)	0.01236(14)	0.00413(8)	0.00048(10)	0.00022(8)
Mg1	0	½	½	0.00903(12)	0.0096(2)	0.0085(2)	0.0089(2)	0.00031(14)	0.00013(17)	0.00024(14)
O1	0.18123(8)	0.60054(8)	0.44825(6)	0.01802(17)	0.0122(4)	0.0228(4)	0.0190(4)	−0.0023(3)	0.0002(3)	0.0079(3)
H1A	0.2575(18)	0.5801(16)	0.4694(12)	0.038(4)*	-	-	-	-	-	-
H1B	0.1911(16)	0.6397(16)	0.3965(12)	0.035(4)*	-	-	-	-	-	-
O2	0.09185(8)	0.31191(8)	0.46467(6)	0.01722(17)	0.0216(4)	0.0110(3)	0.0190(4)	0.0017(3)	0.0070(3)	0.0001(3)
H2A	0.1412(17)	0.3032(16)	0.4136(13)	0.040(4)*	-	-	-	-	-	-
H2B	0.0637(18)	0.2357(18)	0.4787(11)	0.043(4)*	-	-	-	-	-	-
O3	−0.08974(9)	0.51120(8)	0.35938(6)	0.01769(18)	0.0257(4)	0.0132(4)	0.0142(4)	0.0010(3)	−0.0075(3)	−0.0005(3)
H3A	−0.1295(16)	0.5787(17)	0.3368(11)	0.037(4)*	-	-	-	-	-	-
H3B	−0.1147(16)	0.4439(17)	0.3304(12)	0.039(4)*	-	-	-	-	-	-
N1	0.5012(9)	0.48403(18)	0.2343(2)	0.0133(7)	0.0164(7)	0.0179(7)	0.006(2)	0.0028(10)	0.001(2)	0.0028(6)
H1C	0.496(3)	0.497(2)	0.1757(11)	0.020*	-	-	-	-	-	-
H1D	0.563(2)	0.427(2)	0.245(2)	0.020*	-	-	-	-	-	-
H1E	0.429(2)	0.454(3)	0.254(2)	0.020*	-	-	-	-	-	-
H1F	0.527(2)	0.5545(17)	0.258(2)	0.020*	-	-	-	-	-	-

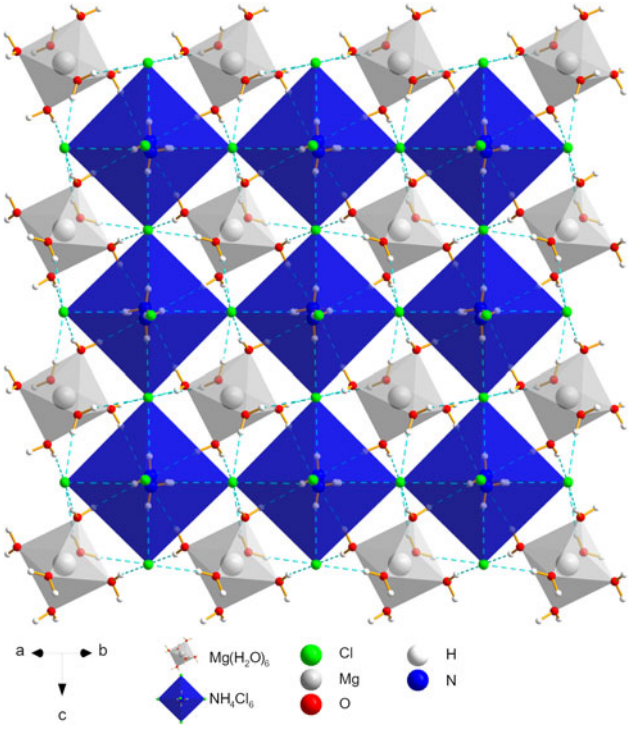

Fig. 5. The crystal structure projection along (110) plane. Corner sharing framework of $NH_4^+Cl_6^-$ octahedra with $[Mg(H_2O)_6]^{2+}$ octahedra filling cavities. Dashed lines indicate hydrogen bonds.

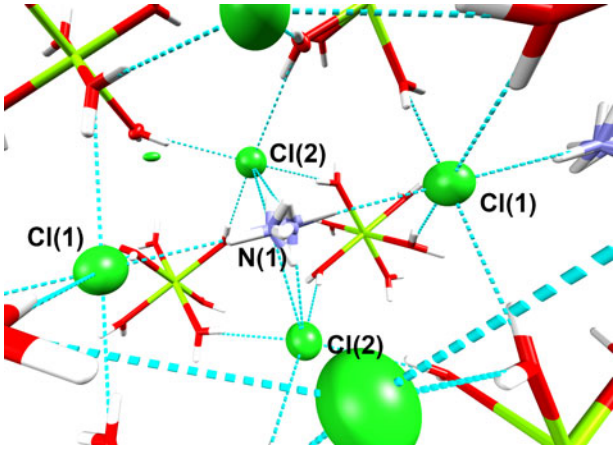

Fig. 6. The magenta dashed lines present a network of hydrogen bond interactions around the NH_4^+ ion (located in the figure centre, violet and white), with water molecules (red and white), and chloride anions (green). Almost overlapping NH_4^+ groups are symmetrically equivalent (by a twofold axis), each being a half occupant.

Table 4. Hydrogen bond lengths (*d* in Å) and angles (in °) for novograblenovite.

D–H···*A*	*d*(*D*–H)	*d*(H···*A*)	*d*(*D*···*A*)	<*DHA*
O1–H1*A*···Cl1	0.785(17)	2.409(17)	3.1814(8)	168.3(15)
O1–H1*B*···Cl2^{i}	0.787(16)	2.380(16)	3.1605(8)	171.1(14)
O2–H2*A*···Cl2^{ii}	0.823(17)	2.347(17)	3.1576(8)	168.4(14)
O2–H2*B*···Cl1^{ii}	0.794(17)	2.341(17)	3.1293(8)	171.8(16)
O3–H3*A*···Cl2^{iii}	0.800(16)	2.357(17)	3.1517(8)	172.3(14)
O3–H3*B*···Cl2^{iv}	0.783(17)	2.405(17)	3.1755(8)	168.2(15)
N1–H1*C*···Cl1^{i}	0.79(1)	2.33(2)	3.114(3)	171(2)
N1–H1*D*···Cl2^{v}	0.80(2)	2.44(2)	3.235(6)	170(3)
N1–H1*E*···Cl2^{ii}	0.77(2)	2.57(2)	3.258(7)	149(3)
N1–H1*F*···Cl2	0.78(2)	2.76(2)	3.428(6)	145(3)

Symmetry codes: (i) $-x+1, y, -z+½$; (ii) $x-½, y-½, z$; (iii) $x-1, y, z$; (iv) $-x+½, y-½, -z+½$; (v) $-x+3/2, y-½, -z+½$.
D – donor of H; *A* – acceptor of H and *d* – interatomic distance.

The Hirshfeld surface approach

The Hirshfeld surface analysis allows for a conceptually simple and straightforward comparison of atomic Hirshfeld volumes within one or many structures (Skovsen *et al.*, 2010; Kastbjerg *et al.*, 2011; Jørgensen *et al.*, 2012). It applies not only to singular atoms but also to multi-atomic ions like NH_4^+ and even the hexaaquamagnesium ion complex, which includes protons from water molecules, in contrast to a simple MgO_6 coordination octahedron volume. The Hirshfeld volumes of cations are summarised in Table 5 and their forms are illustrated in Fig. 7. The K^+ in novograblenovite was calculated by substituting for NH_4^+ in the nitrogen position; all other structural parameters remain unchanged. More space is taken up than for potassium in carnallite (Table 5) suggesting that this ion is less tightly bound in novograblenovite, which also confirms the average K···Cl bond lengths of 3.33 Å *vs.* 3.24 Å of novograblenovite and carnallite respectively. The space of *ca.* 33 Å^3 occupied by NH_4^+ in novograblenovite is

https://doi.org/10.1180/mgm.2020.105 Published online by Cambridge University Press

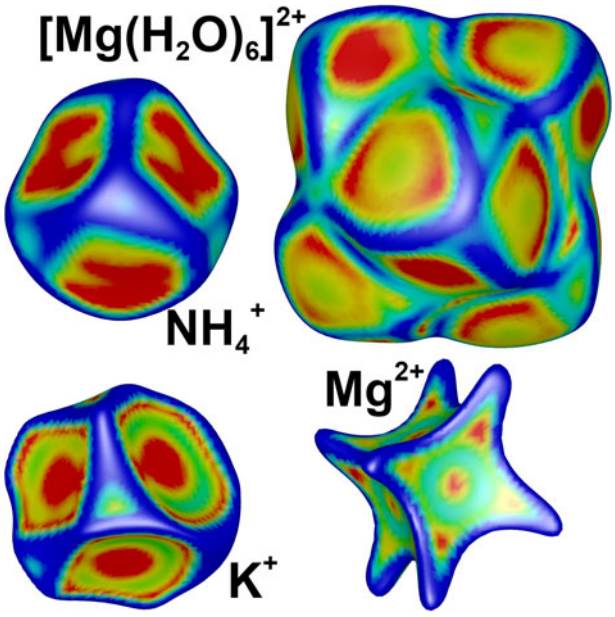

Fig. 7. Curvedness mapped from –1.5 (flat; red) to –0.5 (sphere-like; blue) and plotted on the ionic Hirshfeld surface of the cations in novograblenovite crystal lattice.

Table 5. Cation Hirshfeld volumes (Å^3) in the crystal structures of Novograblenovite and carnallite. Voids were estimated as void volumes (0.002 au) divided by the unit cell volumes.

	Novograblenovite	Carnallite
NH_4^+	33.32	–
K^+	38.37*	33.08 | 30.77
Mg^{2+}	11.54	10.71 | 10.19
$[Mg(H_2O)_6]^{2+}$	160.21	147.43
Voids	13.8%	8.4%

*Corresponding volume of K^+ when substituting NH_4^+

nearly identical to K^+ in carnallite. The curvature is plotted on the Hirshfeld surfaces of ions and is a measure of shape. It is mapped from –1.5 to –0.5 au^{-1}. The maps of curvedness are dominated by a cyan-green colour on a spherical shape, separated by dark blue edges. Highlights of yellow to red indicate flat regions resulting from close contact to another Hirshfeld surface ie. an interaction. This leads to information about the number of nearest neighbours or the coordination sphere of atom or ion (McKinnon *et al.*, 2004).

The void space in the structures of novograblenovite and carnallite are illustrated in Fig. 8, taking up 14% and 8% of the unit cell volume respectively (Table 5). The method can also be applied to studying the porosity of crystalline materials and calculating the volume for an isosurface of 0.0003 au (Turner *et al.*, 2011); however, neither of the analysed minerals is porous.

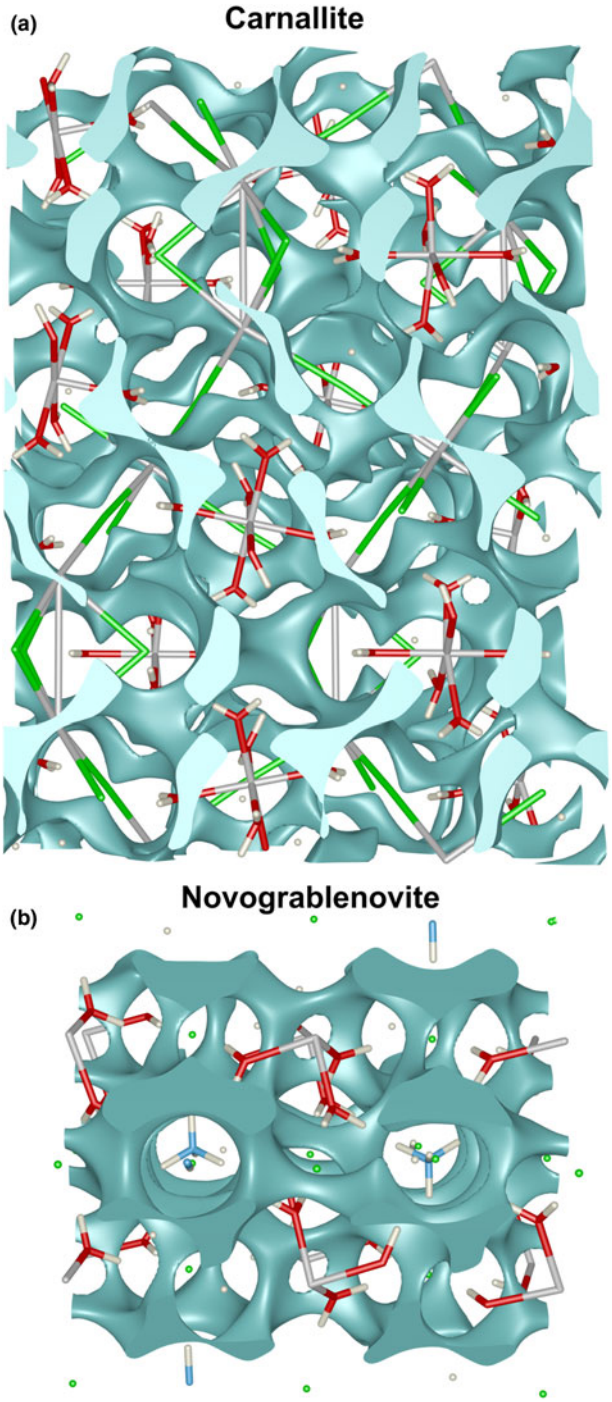

Fig. 8. Procrystal isosurfaces (pastel mint), isovalue of 0.002 au indicating crystal voids in carnallite, projection along [001] (a) and novograblenovite, projection along [110] (b). Atoms are N (blue), H (white), O (red), Mg (grey), Cl (green), K (grey).

Summary

The burning coal-dump at Radlin (Upper Silesia, Poland) stores only rock material from the underground workings of a nearby coal mine. It contains no admixture of municipal or industrial wastes. Therefore, phases formed by spontaneous combustion on this dump fully meet the criteria of the new IMA–CMMC guidelines and should be considered as minerals (Parafiniuk and Hatert, 2020). A mineralogical and structural study of a phase found in significant amounts at Radlin coal dump indicates clearly that it is exactly the same mineral as novograblenovite, described recently from a volcanic exhalation in Kamchatka, Russia (Okrugin *et al.*, 2019). The material discussed in this work forms larger, better developed crystals than those from the volcanic environment which allows us to characterise them more accurately. It does not contain potassium and is close to the chemical formula $NH_4MgCl_3{\cdot}6H_2O$. Novograblenovite from

https://doi.org/10.1180/mgm.2020.105 Published online by Cambridge University Press

Radlin is also analogous to a phase described from burning coal dumps in Chelabinsk, Russia and informally named 'redikortsevite'. Therefore this name should be abandoned.

Our material also enabled us to perform a more detailed structural analysis than for specimens forming in volcanic exhalations. Procrystal electron density analysis was applied with the use of Hirshfeld surfaces that allows a detailed comparison of interactions in the crystal lattices of novograblenovite and its potassium analogue carnallite. It provided information on void space and its visualisation based on the electron-density distribution. Applicability of this fast and simple method may also be of interest in studies involving mineral transformations resulting from the exclusion of water of crystallisation from the crystal lattice. Any other characteristics related to mobility in solid crystalline materials, like clathrates, studies of porosity, comparison of sizes and interactions occupied by trapped ions or molecules, can also take advantage of the approach presented by the example of novograblenovite.

Acknowledgements. KW acknowledges a financial support within the Polish National Science Centre (NCN) OPUS17 grant number DEC-2019/33/ B/ST10/02671. The authors thank Peter Leverett and two anonymous reviewers for very helpful comments on the original manuscript and Stuart Mills, Mihoko Hoshino and Helen Kerbey for their careful editorial handling of the paper.

Supplementary material. To view supplementary material for this article, please visit https://doi.org/10.1180/mgm.2020.105

References

Bader R.F.W. (1994) *Atoms in Molecules: A Quantum Theory*. Clarendon Press, Oxford, UK, 438 pp.

Bader R.F.W., Henneker W.H. and Cade P.E. (1967) Molecular charge distributions and chemical binding. *The Journal of Chemical Physics*, **46**, 3341–3363.

Chang T.G. and Irish D.E. (1973) Raman and infrared spectra study of magnesium nitrate-water systems. *The Journal of Physical Chemistry*, **77**, 52–57.

Chesnokov B., Bazhenova L., Shcherbakova E., Michal T. and Deriabina T. (1988) New minerals from the burned dumps of the Chelyabinsk coal basin. Mineralogy, technogenesis and mineral-resource complexes of the Urals. *Akademiya Nauk SSSR–Uralskoye Otdeleniye*, **5**, 31 [in Russian].

Clementi E. and Roetti C. (1974) Roothaan-Hartree-Fock atomic wavefunctions: Basis functions and their coefficients for ground and certain excited states of neutral and ionized atoms, Z≤ 54. *Atomic Data and Nuclear Data Tables*, **14**, 177–478.

Coppens P. (1997) *X-Ray Charge Densities and Chemical Bonding*. Oxford University Press, Oxford, UK, 384 pp.

Dolomanov O.V., Bourhis L.J., Gildea R.J., Howard J.A.K. and Puschmann H. (2009) OLEX2: a complete structure solution, refinement and analysis program. *Journal of Applied Crystallography*, **42**, 339–341.

Falk M. and Knop O. (1973) Water in stoichiometric hydrates. Pp. 55–113 in: *Water in Crystalline Hydrates Aqueous Solutions of Simple Nonelectrolytes* (F. Franks, editor). Water, Springer Boston, USA.

Haas C. and Hornig D. (1960) Inter-and Intramolecular Potentials and the Spectrum of Ice. *The Journal of Chemical Physics*, **32**, 1763–1769.

Hornig D., White H. and Reding F. (1958) The infrared spectra of crystalline H_2O, D_2O and HDO. *Spectrochimica Acta*, **12**, 338–349.

Jambor J.L. and Puziewicz J. (1993) New Mineral Names. *American Mineralogist*, **78**, 450–455.

Jørgensen M.R.V., Skovsen I., Clausen H.F., Mi J.-L., Christensen M., Nishibori E., Spackman M.A. and Iversen B.B. (2012) Application of atomic Hirshfeld surface analysis to intermetallic systems: is Mn in cubic $CeMnNi_4$ a thermoelectric rattler atom? *Inorganic Chemistry*, **51**, 1916–1924.

Kastbjerg S., Uvarov C.A., Kauzlarich S.M., Nishibori E., Spackman M.A. and Iversen B.B. (2011) Multi-temperature synchrotron powder x-ray diffraction study and Hirshfeld surface Analysis of chemical bonding in the thermoelectric Zintl phase $Yb_{14}MnSb_{11}$. *Chemistry of Materials*, **23**, 3723–3730.

Kruszewski Ł., Fabiańska M.J., Ciesielczuk J., Segit T., Orłowski R., Motyliński R., Kusy D. and Moszumańska I. (2018) First multi-tool exploration of a gas-condensate-pyrolysate system from the environment of burning coal mine heaps: An in situ FTIR and laboratory GC and PXRD study based on Upper Silesian materials. *Science of the Total Environment*, **640–641**, 1044–1071.

Larkin P. (2011) *Infrared and Raman Spectroscopy; Principles and Spectral Interpretation*. Elsevier, 240 pp.

Majzlan J., Schlicht H., Wierzbicka-Wieczorek M., Giester G., Pöllmann H., Brömme B., Doyle S., Buth G. and Bender Koch C. (2013) A contribution to the crystal chemistry of the voltaite group: solid solutions, Mössbauer and infrared spectra, and anomalous anisotropy. *Mineralogy and Petrology*, **107**, 221–233.

Marsh R.E. (1992) Structure of $MgCl_2{\cdot}RbCl{\cdot}6H_2O$. Corrigendum. *Acta Crystallographica*, **C48**, 218–219.

McKinnon J.J., Spackman M.A. and Mitchell A.S. (2004) Novel tools for visualizing and exploring intermolecular interactions in molecular crystals. *Acta Crystallographica*, **B60**, 627–668.

Nakamoto K. (2008) *Infrared and Raman Spectra of Inorganic and Coordination Compounds*. John Wiley & Sons, Inc., Hoboken, New Jersey, USA.

Okrugin V.M., Kudaeva S.S., Karimova O.V., Yakubovich O.V., Belakovskiy D.I., Chukanov N.V., Zolotarev A.A., Gurzhiy V.V., Zinovieva N.G., Shiryaev A.A. and Kartashov P.M. (2017) Novograblenovite, IMA 2017-060. CNMNC Newsletter No. 39, October 2017, page 1284; *Mineralogical Magazine*, **81**, 1279–1286.

Okrugin V.M., Kudaeva S.S., Karimova O.V., Yakubovich O.V., Belakovskiy D.I., Chukanov N.V., Zolotarev A.A., Gurzhiy V.V., Zinovieva N.G., Shiryaev A.A. and Kartashov P.M. (2019) The new mineral novograblenovite, $(NH_4,K)MgCl_3{\cdot}6H_2O$ from the Tolbachik volcano, Kamchatka, Russia: mineral description and crystal structure. *Mineralogical Magazine*, **83**, 223–231.

Parafiniuk J. and Hatert F. (2020) New IMA CNMNC guidelines on combustion products from burning coal dumps. *European Journal of Mineralogy*, **32**, 215–217.

Pekov I.V., Krivovichev S.V., Yapaskurt V.O., Chukanov N.V. and Belakovskiy D.I. (2014) Beshtauite, $(NH_4)_2(UO_2)(SO_4)_2{\cdot}2H_2O$, a new mineral from Mount Beshtau, Northern Caucasus, Russia. *American Mineralogist*, **99**, 1783–1787.

Pye C.C. and Rudolph W.W. (1998) An *ab initio* and Raman investigation of magnesium(II) hydration. *The Journal of Physical Chemistry A*, **102**, 9933–9943.

Schlemper E.O., Gupta P.K.S. and Zoltai T. (1985) Refinement of the structure of carnallite, $Mg(H_2O)_6KCl_3$. *American Mineralogist*, **70**, 1309–1313.

Sheldrick G.M. (2008) A short history of *SHELX*. *Acta Crystallographica*, **A64**, 112–122.

Sheldrick G.M. (2015) Crystal structure refinement with SHELXL. *Acta Crystallographica*, **C71**, 3–8.

Sindern S., Warnsloh J., Witzke T., Havenith V., Neef R. and Etoundi Y. (2005) Mineralogy and geochemistry of vents formed on the burning coal mining waste dump Anna I, Alsdorf, Germany. *European Journal of Mineralogy*, **17**, 130.

Skovsen I., Christensen M., Clausen H.F., Overgaard J., Stiewe C., Desgupta T., Mueller E., Spackman M.A. and Iversen B.B. (2010) Synthesis, crystal structure, atomic Hirshfeld surfaces, and physical properties of hexagonal $CeMnNi_4$. *Inorganic Chemistry*, **49**, 9343–9349.

Solans X., Font-Altaba M., Aguiló M., Solans J. and Domenech V. (1983) Crystal form and structure of ammonium hexaaquamagnesium trichloride, $NH_4[Mg(H_2O)_6]Cl_3$. *Acta Crystallographica*, **C39**, 1488–1490.

Spackman M.A. (2013) Molecules in crystals. *Physica Scripta*, **87**, 048103.

Spackman M.A. and Jayatilaka D. (2009) Hirshfeld surface analysis. *CrystEngComm*, **11**, 19–32.

Spek A.L. (2003) Single-crystal structure validation with the program *PLATON*. *Journal of Applied Crystallography*, **36**, 7–13.

Stachowicz M., Malinska M., Parafiniuk J. and Woźniak K. (2017) Experimental observation of charge-shift bond in fluorite CaF_2. *Acta Crystallographica*, **B73**, 643–653.

Stracher G.B., Prakash A., Schroeder P., McCormack J., Zhang X., Van Dijk P. and Blake D. (2005) New mineral occurrences and mineralization processes:

Wuda coal-fire gas vents of Inner Mongolia. *American Mineralogist*, **90**, 1729–1739.

Turner M.J., McKinnon J.J., Jayatilaka D. and Spackman M.A. (2011) Visualisation and characterisation of voids in crystalline materials. *CrystEngComm*, **13**, 1804–1813.

Turner M.J., McKinnon J.J., Wolff S.K., Grimwood D.J., Spackman P.R., Jayatilaka D. and Spackman M.A. (2017) *CrystalExplorer17*. University of Western Australia, Australia.

Žáček V. and Ondruš P. (1997) Mineralogy of recently formed sublimates from Kateřina colliery in Radvanice, Eastern Bohemia, Czech Republic. *Věstník Českého geologického ústavu*, **72**, 289–302.

Zolotarev A.A., Zhitova E.S., Krzhizhanovskaya M.G., Rassomakhin M.A., Shilovskikh V.V. and Krivovichev S.V. (2019) Crystal chemistry and high-temperature behaviour of ammonium phases $NH_4MgCl_3{\cdot}6H_2O$ and $(NH_4)_2Fe^{3+}Cl_5{\cdot}H_2O$ from the burned dumps of the Chelyabinsk coal basin. *Minerals*, **9**, 486.

https://doi.org/10.1180/mgm.2020.105 Published online by Cambridge University Press